journal of the mechanical behavior of biomedical materials 151 (2024) 106353

Contents lists available at ScienceDirect

Journal of the Mechanical Behavior of Biomedical Materials

journal homepage: www.elsevier.com/locate/jmbbm

Light transmittance through resin-matrix composite onlays adhered to resin-matrix cements or flowable composites

Rita Fidalgo-Pereira [a], Susana O. Catarino [b,c], Óscar Carvalho [b,c], Nélio Veiga [a], Orlanda Torres [d], Annabel Braem [e], Júlio C.M. Souza [a,b,c,*]

[a] Center for Interdisciplinary Research in Health (CIIS), Faculty of Dental Medicine (FMD), Universidade Católica Portuguesa (UCP), 3504-505, Viseu, Portugal
[b] Center for MicroElectroMechanical Systems (CMEMS-UMinho), University of Minho, 4800-058, Guimarães, Portugal
[c] LABBELS - Associate Laboratory, University of Minho, Guimarães, 4710-057 Braga, Portugal
[d] Oral Pathology and Rehabilitation Research Unit (UNIPRO), University Institute of Health Sciences (IUCS), CESPU, 4585-116 Gandra, Portugal
[e] Department of Materials Engineering (MTM), Biomaterials and Tissue Engineering Research Group, KU Leuven, 3000 Leuven, Belgium

ARTICLE INFO

Keywords:
Optical transmittance
Resin cements
Resin-matrix composites
Thickness
Polymerization

ABSTRACT

Objective: The aim of this study was to evaluate the influence of the thickness of resin-matrix composite blocks manufactured by CAD-CAM on the light transmittance towards different resin-matrix cements or flowable composites.

Methods: Sixty specimens of resin-matrix composite CAD-CAM blocks reinforced with 89 wt% inorganic fillers were cross-sectioned with 2 or 3 mm thicknesses. The specimens were conditioned with adhesive system and divided in groups according to the luting material, namely: two dual-cured resin-matrix cements, two traditional flowable resin-matrix composites, and one thermal-induced flowable resin-matrix composite. Specimens were light-cured at 900 mW/cm^2 for 40s. Light transmittance assays were preformed using a spectrophotometer with an integrated monochromator before and after light-curing. Microstructural analysis was performed by optical and scanning electron microscopy (SEM). Nanoindentation tests were performed to evaluate mechanical properties for indirect evaluation of degree of monomers conversion.

Results: Optical and SEM images revealed low thickness values for the cementation interfaces for the traditional flowable resin-matrix composite. The cement thickness increased with the size and content of inorganic fillers. The highest light transmittance was recorded for the onlay blocks cemented with the traditional flowable resin-matrix composites while a group cemented with the dual-cured resin-matrix cement revealed the lowest light transmittance. The elastic modulus and hardness increased for specimens with high content of inorganic fillers as well as it increased in function of the light transmittance.

Conclusions: The light transmittance of flowable resin-matrix composites was higher than that for resin-matrix cement after cementation to resin-matrix composites blocks. The type, size, and content of inorganic fillers of the luting material affected the thickness of the cement layer and light transmittance through the materials.

Clinical relevance: On chair-side light curing, the transmission of visible light can be interfered by the chemical composition and viscosity of the luting materials. The increase in size and content of inorganic fillers of resin-matrix composites and luting materials can decrease the light transmittance leading to inefficient polymerization.

1. Introduction

Nowadays, several types of indirect restorative composites or ceramics are often cemented with luting materials such as resin-matrix composite cements (Oh et al., 2018a; Mendonça et al., 2019; Fidalgo--Pereira et al., 2023). Thus, the clinical performance of the restorative interfaces depends on the polymerization of the luting materials (Lise et al., 2018a; Tafur-Zelada et al., 2021). On the contrary, an unproper polymerization cause mechanical failures of the luting interface and debonding of the restorative material that can lead to the following clinical issues: marginal discoloration, catastrophic fractures, microleakage, secondary caries, and operative sensitivity with patient'

* Corresponding author.
E-mail addresses: jsouza@dem.uminho.pt, jsouza@ucp.pt (J.C.M. Souza).

https://doi.org/10.1016/j.jmbbm.2023.106353
Received 15 November 2023; Received in revised form 21 December 2023; Accepted 24 December 2023
Available online 28 December 2023

discomfort (Oh et al., 2018a; Fidalgo-Pereira et al., 2023; Kim et al., 2013; Hardy et al., 2018).

Currently, resin-matrix cements are mainly composed of a polymeric matrix embedding inorganic fillers as follow: silica, zirconia, zirconium silicate, barium glass, strontium calcium aluminosilicate glass, quartz, or ytterbium fluoride (Oh et al., 2018a; Mendonça et al., 2019; Fidalgo-Pereira et al., 2023; Fidalgo-Pereira et al., 2023; Tafur-Zelada et al., 2021; Ioannidis et al., 2019; Gultekin et al., 2015). The polymeric (organic) matrix is often composed of bisphenol A-glycidyl dimethacrylate (Bis-GMA), urethane dimethacrylate (UDMA), and triethylene glycol dimethacrylate (TEGDMA) (Fidalgo-Pereira et al., 2023; Tafur--Zelada et al., 2021; Ioannidis et al., 2019; Gultekin et al., 2015). Commercially available resin-matrix cements have an inorganic content that varies from 57 up to 78 wt % (Fidalgo-Pereira et al., 2023; Ferracane et al., 2011; Valentini et al., 2014; Santi et al., 2022). The inorganic particles of the resin-matrix cements can show irregular or spherical shape, with sizes ranging from 0.5 up to 20 μm (Aguiar et al., 2012; Barbon et al., 2022). The size and content of fillers determine the physical properties of the materials. The polymeric matrix of resin-matrix cements can involve chemical and light-induced initiators which are stimulated to promote the polymerization of the polymeric matrix (Lise et al., 2018a; Tafur-Zelada et al., 2021). A similar chemical composition can be noted for resin-matrix composites utilized for dental restorations although some specific molecules can be detected within the organic matrix of the self-adhesive cements for enhanced adhesion such as: 10-Methacryloyloxydecyl dihydrogen phosphate (10-MDP).

Dual-cured resin-matrix cements involve both chemical and light-induced polymerization that is the first-choice for a broad range of procedures with indirect restorations (De Souza et al., 2015; Gheller et al., 2020) (Fidalgo-Pereira et al., 2023; Alkhudhairy et al., 2020). The chemical reaction involves the combination between the benzoyl peroxide and a tertiary amine while a phototoinitiator compound (i.e., camphorquinone) is stimulated by visible light irradiation at around 420 and 490 nm (Franken et al., 2019; David-Pérez et al., 2022; Chen et al., 2019; Fidalgo-Pereira et al., 2022; Delgado et al., 2019). An adequate degree of conversion (DC) of monomers in resin-matrix cements under an indirect restoration must be achieved between 55 and 75% to ensure proper physical and biologic properties (Butler et al., 2021; De Souza et al., 2015; Moldovan et al., 2019; Xu et al., 2020; Ling et al., 2022). Several factors can affect the DC of a resin-matrix cement such as: (i) light attenuation of indirect restorations, due to the microstructure, opacity and thickness; (ii) light curing units (LCU), procedures, light irradiance, light exposure time, visible light wavelength, distance between LCU and the resin-matrix cement; (iii) organic matrix type, fillers's size and content, and refraction index of organic and inorganic components (Mendonça et al., 2019; Faria and Pfeifer, 2017; Kelch et al., 2022a; Valentino et al., 2010; Bragança et al., 2020; Ling et al., 2022; Yoshida and Meng, 2014).

Even though indirect restorations can be manufactured from zirconia or lithium disilicate-reinforced glass ceramics, resin-matrix composite blocks manufactured by CAD-CAM become an alternative material due their technological developments in recent years (Mendonça et al., 2019; Kim et al., 2013; Hardy et al., 2018; Zimmermann et al., 2019; Magalhães et al., 2023). Resin-matrix composites have elastic modulus, fracture toughness, and strength quite similar to that recorded at the dentin-enamel junction tissues (Goldberg et al., 2016; Magne and Knezevic, 2009; Kameyama et al., 2015; Fidalgo-Pereira et al., 2023). Also, resin-matrix composites show versatile optical properties depending on the chemical composition and microstructure (Hardy et al., 2018; Kameyama et al., 2015). Thus, the chemical composition, opacity, shade, and thickness of the indirect restoration material affect the optical transmittance through the resin-matrix cement (Mazzitelli et al., 2022; Sulaiman et al., 2015; Blumentritt et al., 2021; Gregor et al., 2014; Meng et al., 2022; Pacheco et al., 2019; Shim et al., 2017). Nevertheless, the thickness of the restorative material, microstructure, and type of resin-matrix cements should be clarified concerning different commercially available materials.

Thus, the aim of this study was to evaluate the light transmittance through resin-matrix composites blocks manufactured by CAD-CAM regarding the use of traditional resin-matrix cements or flowable resin-matrix composites. The null hypothesis is that there are no light transmittance changes considering the type of luting material neither due to the thickness of the restorative material.

2. Materials and methods

2.1. Preparation of specimens

Resin-matrix composites specimens were manufactured from Grandio Blocs™ blocks (VOCO, Germany) with dimensions at 18 × 14.5 × 14.8 mm. The chemical composition and general features of the material are described in Table 1. The resin-matrix composite blocks were cross-sectioned at low-speed using a diamond disc coupled to an automated water-cooled precision cutting machine (Minitron Stuers A/S, Denmark) (Sadighpour et al., 2018). Sixty resin-matrix composites square specimens (6 × 6 mm) were produced with two different thickness, namely 2 and 3 mm. The preparation and analysis of the specimens is shown in Fig. 1. After cutting, specimens were ultrasonically rinsed in isopropyl alcohol for 10 min and then in distilled water for 10 min. The inner surfaces of the onlays were conditioned with a silane compound (Ceramic bond™, VOCO GmbH, Cluxhaven, Germany) over a period of 60 s, then gently oil-free air dried for 5 s following the manufacturer's instructions (Mendonça et al., 2019; Turp et al., 2015). The inner surfaces of the specimens were conditioned with a universal adhesive (Futurabond M + ™, VOCO, Germany) at reciprocating sliding motion using a microbrush for 20 s following the manufacturer's instructions (Magalhães et al., 2023). An oil-free air was applied onto the adhesive layer for 5 s to remove the adhesive solvents and then the specimens were attached into a polyvinyl chloride mold to provide a mechanical stability over the cementation procedure (Mendonça et al., 2019; Turp et al., 2015).

On the cementation, two traditional dual-cured resin-matrix cements containing 73 wt% (73%B; Bifix QM™, VOCO, Germany) or 78 wt% (78%P; Panavia F™, Kuraray, Japan) inorganic fillers were assessed. Furthermore, two traditional flowable resin-matrix composites (83%Hf, GrandioSO Heavy Flow ™, and 60%Lf, GrandioSO Light Flow ™; VOCO, Germany) and a thermally-induced flowable resin-matrix composite (TI83%V; VisCalor bulk™, VOCO, Germany), were assessed in this study for comparison with the resin-matrix cements. The thermally-induced flowable resin-matrix composite (VisCalor bulk™, VOCO, Germany) was heated up to 61 °C for 2.5 min using a hand-held dispenser, namely Caps Warmer™ (VOCO, Germany) following the manufacturer's recommendations to attain a flowable consistency for cementation (Acquaviva et al., 2009).

The resin-matrix cements and composites were applied onto each specimen' surface on 9.807 N axial loading using a 1 kg weight through the dental inspector apparatus for 60 s, as seen in Fig. 1. A silicone key and the dental inspector apparatus were used to guarantee a positioning stability avoiding horizontal displacement of the specimen (Sadighpour et al., 2018; Tekçe et al., 2018; Magalhães et al., 2023). The excessive amount of the cement was removed using a microbrush.

At last, the polymerization of luting materials was carried out using a Light Emitting Diode (LED) light curing unit (Smartlite™ Focus™, Dentsply, Germany). The light curing unit (LCU) provided visible light at a wavelength ranging from 420 up to 540 nm and irradiance of 900 mW/cm^2. Prior to the polymerization procedure, the irradiance was verified using a calibrated radiometer (Proclinic Expert™, Montellano, Portugal) avoiding any probability of low irradiance over the specimens. The LCU tip was positioned in contact with the specimen to maintain a standard source distance (Rode et al., 2007; Magalhães et al., 2023; Fidalgo--Pereira et al., 2023). The manufacturer's specifications of the luting materials can be seen in Table 1.

Table 1
Chemical composition of the resin-matrix composites blocks manufactured by CAD-CAM, adhesive systems, and luting materials.

Group; material (brand, manufacturer, country)	Organic matrix	Inorganic Fillers % (w/w)	Inorganic Fillers % (v/v)	Filler shape and type
Onlay; Resin-matrix composites blocks manufactured by CAD-CAM (n.o 14 L and dimensions with 18 × 14.5 × 14.8 mm) (GrandioSO ™ , VOCO GmbH, Germany)	Bis-GMA, Bis-EMA, TEGDMA	89	73	Micro-scale barium glass and zirconium glass ceramics particles: 0.5–3 μm. Nano-scale SiO_2 particles: ~40 nm
Adhesive; Universal adhesive system (Futurabond M + ™, VOCO GmbH, Germany)	Organophosphate monomer (10-MDP), Methacrylates (2-HEMA, bis-GMA, UDMA), ethanol, catalyst, pyrogenic silicic acids, BHT, water	–	–	Functionalized nano-scale SiO_2 particles: 20 nm
73%B; Dual curing, adhesive resin-matrix cement (Bifix QM™, VOCO, GmbH, Germany)	DMA, Bis-GMA, benzoyl peroxide, amines	71–73	61	Micro-scale barium-aluminum-boro-silicate glass ceramic and nano-scale amorphous silica fillers
78%P; Dual curing resin-matrix cement (Panavia F™, Kuraray, Japan)	Bis-GMA, TEGDMA, Bis-EMA	78	59	Micro-scale barium glass ceramic, fluor-aluminum-silicate glass ceramic, and aluminum oxide particles. Functionalized nano-scale SiO_2 particles. Average particle size: 0.04–12 μm.
83%Hf; Flowable resin-matrix composite, GrandioSO (Heavy Flow™, VOCO GmbH, Germany)	Bis-GMA, Bis-EMA, TEGDMA, HDDMA, CQ, amine and BHT	83	68	Micro-scale barium glass ceramic and zirconium glass ceramic particles at 1 μm. Nano-scale SiO_2 particles at 20–40 nm
60%Lf; Flowable resin-matrix composite (GrandioSO Light Flow ™, VOCO GmbH, Germany)	TEGDMA, Bis-GMA	60	37	Amorphous silica and zinc oxide particles at around 0.02–1.5 μm
TI83%V; Thermally induced resin-matrix composite (VisCalor bulk™, VOCO GmbH, Germany)	Bis-GMA, aliphatic dimethacrylate	83	68	Micro-scale barium glass ceramic and zirconium glass ceramic micro-scale particles at 1 μm. Nano-scale SiO_2 particles at around 20–40 nm

Organic compounds: Bisphenol A-glycidyl dimethacrylate (Bis-GMA), urethane dimethacrylate (UDMA), and triethylene glycol dimethacrylate (TEGDMA), Ethoxylated bisphenol A dimethacrylate (Bis-EMA), butylated hydroxytoluene (BHT), camphorquinone (CQ), dimethacrylate (DMA), Hydroxyethylmethacrylate (HEMA), 1,6 - Hexanediol dimethacrylate (HDDMA).

Groups of resin-matrix composite onlay specimens were also cemented over human dentin to provide an interface for nano-indentation and microscopy assays. Twenty extracted third molars retrieved from human participants were initially submerged in distilled water for 10 min and then in a solution of 2% sodium hypochlorite (NaOCl) for 10 min. Afterwards, teeth were immersed in 10% formalin solution for 1 week. Finally, teeth will be stored in 0.9% NaCl solution for rehydration over a period of 7 days prior to the cementation procedure. That procedure was carried out following ISO 4882:20,015 guidelines (González-Colmenares et al., 2020; Goel et al., 2013; Magalhães et al., 2023). The handling of extracted third molars was approved by the Human Research Ethics Committee at the University Institute of Health Sciences, reference number 13/CE-IUCS/-CESPU/2022, that is in agreement with the Helsinki declaration of 1964. The participants signed the informed consent prior to inclusion in the project since the objective of the project was described. The participants did not suffer from any systemic disease and therefore they showed worthy oral health, free of antibiotic therapy over the last 24 weeks.

On the tooth preparation, the root and coronal portions were removed and then the enamel was removed from all the surfaces using a conical trunk diamond bur with 1.2 mm diameter. Dentin slides were prepared and surfaces were finished using a 1.5 mm cylindrical diamond bur. Then, dentin surfaces were etched with phosphoric acid 37% (Clarben SA, Spain) for 15 s and rinsed with distilled water for 30 s. Dentin slices were placed into the polyvinyl chloride mold and the surfaces were dried with cotton and then conditioned using an universal adhesive prior to the cementation with the luting materials. The luting materials were placed over the resin-matrix composite onlay specimens and positioned over the dentin surfaces and then the loading of 9.807 N (1 kg) was applied on the top of the resin-matrix composite onlay hold by the dental apparatus (Straface et al., 2019; Zhang et al., 2019). Specimens were light cured at 900 mW/cm^2 using the LCU for 60 s (Souza et al., 2014; Magalhães et al., 2023) and embedded in autopolymerizing polyether (Technovit 400™, Kulzer, GmbH, Germany) for cross-section at a 90° angle, relative to the interface plane. The cross-sectioning was carried out by wet grinding on SiC papers (Trizact™, 3 M ESPE, USA) from 380 down to 2400 mesh, followed by polishing with 300 and 6000 mesh (3 μm particle size) SiC papers (Fidalgo-Pereira et al., 2023; Magalhães et al., 2023). Then, specimens were ultrasonically cleaned in prophyl alcohol for 5 min and in distilled water for 10 min (El-Safty et al., 2012).

2.2. Chemical and microscopic assays

Cross-sectioned specimens were inspected using a Leica DM 250 ™ optical microscope (Leica Microsystems, Germany). The microscope was attached to a computer for image processing via Leica Application Suite™ software (Leica Microsystems, Germany), with a magnification ranging from × 30 up to × 1.000. Adobe Photoshop ™ (Adobe Systems Software, Ireland) was used to analyze the restorative interfaces and the organic matrix (white images) and inorganic filler particles (black images). The dimensions of the cement layer and the inorganic filler particles' size were measured by ImageJ™ (National Institutes of Health, USA) software, as shown in Fig. 2. The measurement of cement layer thickness was performed perpendicularly to the interface plane although the interface follows the contours of the tooth and onlay cementation surfaces.

The surfaces were previously sputter coated with a silver palladium (AgPd) alloy for scanning electron microscopy (SEM) analysis. The specimens' microstructure and their interfaces were evaluated at high magnification, ranging from × 1.000 up to × 20.000, under secondary (SE) and backscattered electrons (BSE), as shown in Fig. 3. SEM images were recorded at magnification ranging from × 30 up to × 20,000 at

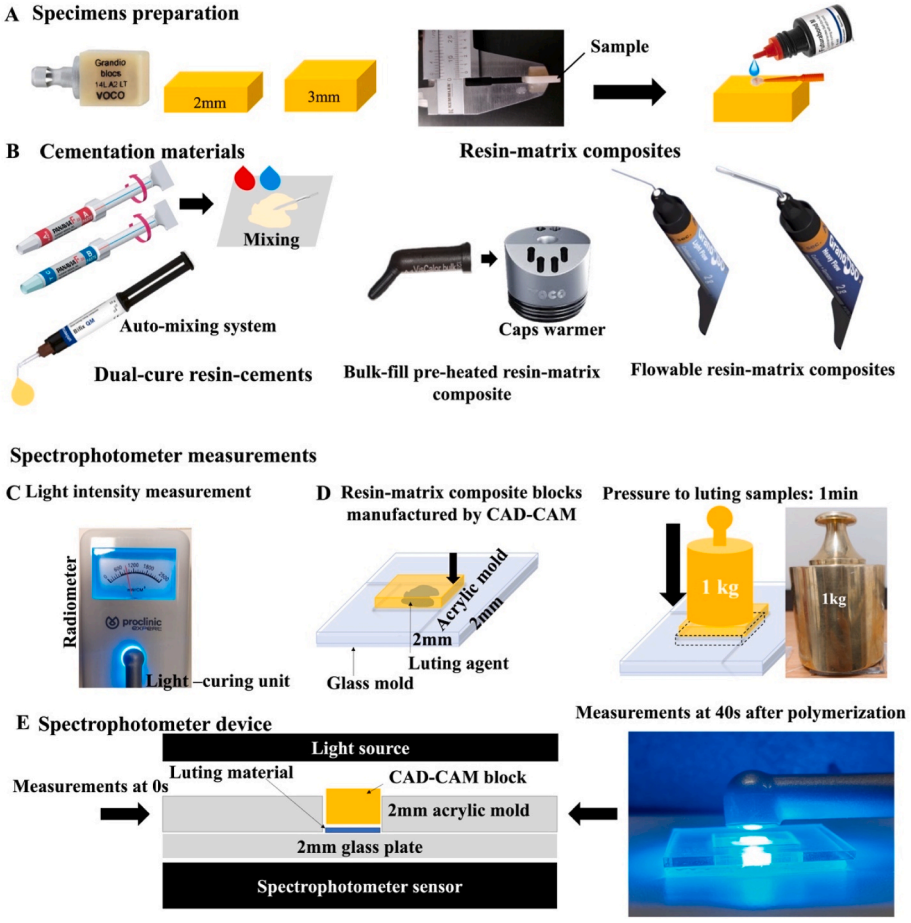

Fig. 1. Specimens prepared from resin-matrix composites blocks and cementation procedure. (A) Specimens' preparation with two thickness and surface conditioning. (B) Materials for cementation. (C) Light curing calibration and (D) positioning of the specimens into acrylic molds. (E) Set tup of the light curing.

three different areas for each sample ($n = 15$). SEM images were acquired using a SEM unit JSM-6010 LV™, JEOL, Japan, coupled to energy dispersive spectroscopy (EDS). Even though the chemical composition of the resin-matrix composites was provided by the manufacturers (in Table 1), elemental analyses were performed by EDS. The chemical composition of the materials was evaluated by EDS using a silicon drift detector energy-dispersive spectrometer (SDD-EDS). The characteristic X-Rays emitted from the atoms are harvested by the SSD, that evaluate the signal considering standard computational data to estimate the atomic fraction.

2.3. Nanoindentation assays

Nanoindentation tests were carried out with the loading axis at 90° relative to the interface plane of the specimens. A table top nano-indentation tester (TTX-NHT™, CSM instruments, Needham, MA, USA) operated with a Berkovich diamond pyramid tip (apex angle of 143°) was used to perform nanoscopic indentations in triplicate over the surfaces ($n = 15$). Load of 5 mN was applied at 0.04 mN/s onto the specimens for 15 s. Six points at different regions along the restorative interface. The shape function was determined by the Oliver & Pharr method (1992). Nanoindentation tests allowed evaluating stress/strain fields induced during indentation across the specimen with respect to the displacement axis of the indenter. Nano-hardness and elastic modulus of the materials were acquired as a function of the positioning of the indenter axis relative to the specimens' interface.

2.4. Optical transmittance

The optical transmittance measurements were performed within a wavelength range between 350 nm and 850 nm, with a measurement integration time of 10 ms, using a top-bench spectrophotometer with an integrated monochromator (AvaSpec-ULS2048XL EVO™, Avantes, NS Apeldoorn, The Netherlands). The apparatus comprised a 200 W Quartz Tungsten Halogen light source (Model 66,881, Oriel Newport, USA), optical-fiber probes, and a metallic holder for specimens, as shown in Fig. 1. The spectrophotometer was coupled to a computer for data acquisition and processing, including smoothing based on 100 measurements' average (1 s overall analysis time). Spectrophotometer has an optical bench with 37.5, 50-, 75- or 100-mm focal length, developed in a symmetrical Czerny-Turner design. A SMA-905 standard connector allows the light entrance on the optical bench of the spectrophotometer, where it is collimated by a spherical mirror. The collimated light was diffracted by a plain grating, while a second spherical mirror focuses resulting in diffracted light. As manufacturer information, an image of the spectrum is projected into a 1-dimensional linear detector array. The experiments were run in triplicate and carried out in five independent assays. The specimens were analyzed before polymerization 0 s (pre-polymerization) and after light-curing for 40 s (post-polymerization), both for the 2-mm and 3-mm thickness specimen sets. The measurements were immediately performed after polymerization. For calibration purposes, optical reference measurements were acquired between each set of measurements. Also, a previous analysis was performed to evaluate the light transmission through the specimens, with the following thickness: 2, 3 and 4 mm.

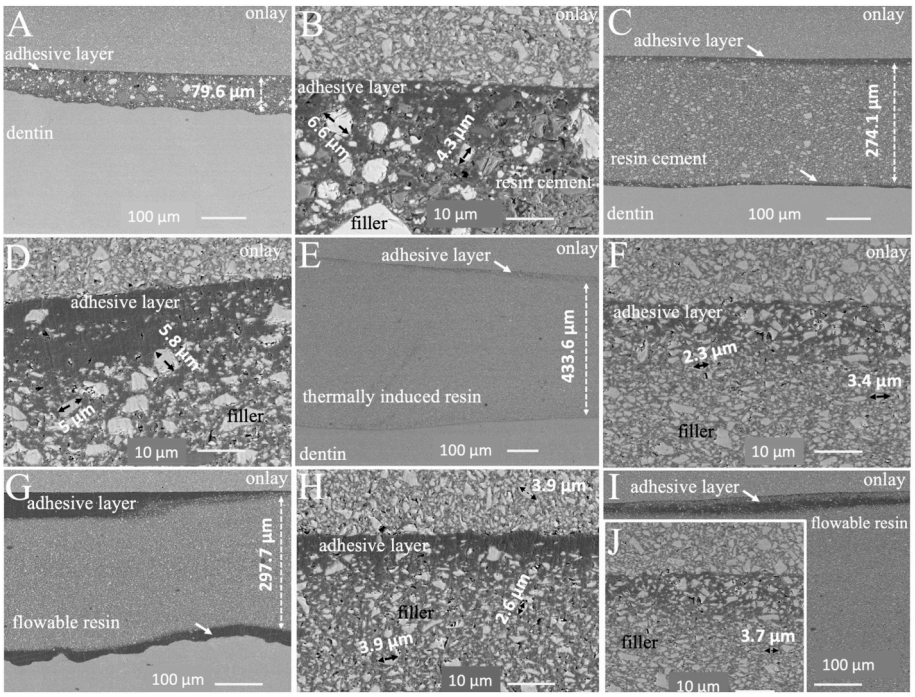

Fig. 2. SEM images acquired for restorative interfaces cemented with resin cements reinforced with (A,B) 78 wt% and (C,D) 73 wt% inorganic fillers (78%P and 73% B groups, respectively). (E,F) SEM images for restorative interfaces cemented with the thermally-induced flowable resin-matrix composited reinforced with 83 wt% inorganic fillers (TI83%V) and for the flowable resin-matrix composited reinforced with (G,H), 60 wt% and (I,J) 83%wt inorganic fillers (60%Lf and 83%Lf groups, respectively). SEM images performed at SE mode and at 15 kV. SEM images at (A,C,E,G,I) × 200 and (B,D,F,H,J) × 2000 magnification.

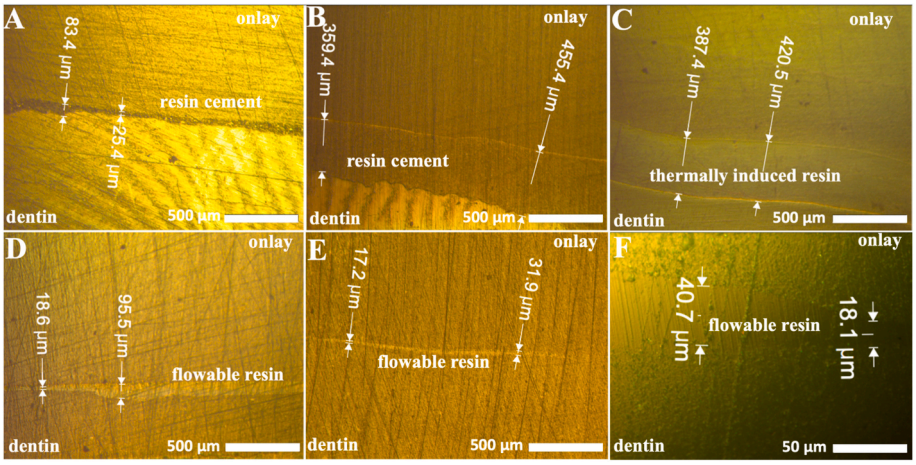

Fig. 3. Optical microscopy (OM) images at × 50 magnification of restorative interfaces cemented with traditional resin-matrix cements reinforced with (A) 78 wt% and (B) 73 wt% inorganic fillers (78%P and 73%B groups, respectively) and for (C) the thermally induced resin-matrix composite (TI83%V). OM images at ×50 for the traditional flowable resin-matrix composited reinforced with (D) 60 wt% and (E) 83 wt% inorganic fillers (60%Lf and 83%Hf groups, respectively) and (F) at × 500 for the 83%Hf group.

2.5. Statistical analysis

The statistical treatment of the data was carried out using the Statistical Package for Social Sciences (SPSSTM) Version 29.0 program, from International Business Machines (IBM, Armonk, NY, USA). Normality tests were applied on the assumption that there was no association or difference between the elements and the variables. The Kolmogorov- Smirnov and Shapiro-Wilk tests were designed to determine whether a sample can be considered to come from a population with a particular distribution. Levene's test was also used to correct the Kolmogorov-Smirnov test when the distribution was normal, thus increasing the power of the test. In this study, the normal distribution of the data was not verified when applying the Kolmogorov—Smirnov test followed by Levene test, where the p-value was set for a significance level of 5% (<0.05). The statistical analyses were carried out by non-parametric statistical tests to determine the statistical differences in nano-hardness, elastic modulus, and transmittance between groups. Kruskal- Wallis tests, and One-Way ANOVA with Bonferroni corrections were performed for multiple comparisons to check the influence of the test solutions within a level of statistical significance (α) at 5%. A power analysis was performed by the t-student test to determine the number of specimens to validate de results, and therefore to disclose a test power of 100% in this study.

3. Results

3.1. Microstructural aspects

The microstructure of the restorative interfaces is shown in Figs. 2 and 3. As seen by SEM analyses, different microstructural features were explored focusing on the dimensions of the restorative interface and inorganic fillers. The resin-matrix cement reinforced with 78 wt% inorganic fillers (78%P) showed larger micro-scale inorganic particles when compared with the other resin-matrix cement (73%B). The micro-scale inorganic fillers of the 78%P group were composed of barium glass or fluoroalminosilicate glass ranging from 1 up to 20 μm. Micro-scale barium-aluminiumboro-silicate glass at around 1–6 μm and nano-scale amorphous silica fillers were detected in the microstructure of 73%B resin-matrix cement. It should be emphasized that the dimensions of the inorganic fillers are proper for enhanced mechanical properties of the restorative interface. The micro-structure of the flowable resin-matrix composites (83%Hf, 60%Lf, and TI83%V) are quite similar considering the chemical composition of the inorganic fillers composed of micro-scale glass ceramic particles at around 1–6 μm and nano-scale amorphous silica at approximately 40 nm. The flowable resin-matrix composite named Ti83%V showed inorganic particles ranging from 0.81 up to 5.5 μm, while the 60%Lf showed particles ranging from 1.37 up to 3.77 μm. In fact, average size of the inorganic fillers was smaller for the flowable composites when compared to the resin-matrix cements. The dimensions of the restorative interface was variable considering the viscosity and chemical composition of the luting materials, as seen in Figs. 2 and 3. The thin layer of the adhesive system can be detected at the restorative interface by SEM analysis (Fig. 2).

The variation in thickness of the cementation layer was noticeable for the restorative interfaces. The mean values of the cementation layer are provided in Table 2. On the resin-matrix cements, thickness values ranged from 25 up to 83 μm for the cement containing 78 wt% inorganic fillers (78%P) while the cement containing 73 wt% inorganic fillers (73%B) showed thickness values at around 359 and 455 μm (Fig. 3A and B). On the traditional flowable resin-matrix composites, the thickness mean values ranged from 18.6 up to 95.5 μm for flowable resin-matrix composite containing 83 wt% inorganic fillers (83%Lf) and from 17.2 up to 32 μm for the flowable composite containing 60 wt % (60%Hf). The thermally induced (TI) resin-matrix composite with 83 wt % inorganic fillers (Ti83%V) revealed thickness values at around 387 and 420 μm (Fig. 3).

3.2. Optical transmittance results

At first, preliminary optical transmittance assays were performed to evaluate the light transmittance through the resin-matrix composite specimens in the absence of resin-matrix cement or flowable resin-matrix composite. The onlay specimens were produced at three different thickness: 2, 3, and 4 mm. The optical transmittance spectra for the specimens free of luting agent are shown in Fig. 4. Regarding the specimens with 2- or 3-mm thickness, the results show that a small amount of light is still transmitted through the onlays. Even for the specimens with 2-mm thickness, less than 0.5 % light is transmitted in the 600–850 nm range through the specimens towards the luting material. As expected, the transmitted light decreases with the increase in thickness of the onlays specimens.

Before polymerization, the 2-mm thickness specimens' behavior was quite similar for all groups, as shown in Fig. 4B and D. Although the plots data from the specimens are superimposed in most of their spectra, the optical transmittance increased above 600 up 850 nm. The highest optical transmittance was recorded for onlays bonded to the thermally induced flowable resin-matrix composite reinforced with 83 wt% inorganic fillers (TI83%V). On the other hand, the lowest optical transmittance value at 850 nm was recorded for the onlays bonded to the resin cement reinforced with 78 wt% inorganic fillers (78%P) (Fig. 4B).

After light curing for 40s, the highest optical transmittance values were recorded for the 2-mm thickness onlays bonded to flowable resin-matrix composites reinforced with 60 or 83 wt% inorganic fillers followed by groups 73%B and TI83%V. The lowest values of optical transmittance were recorded for 78%P that was quite similar to the results before polymerization. Regarding the 2-mm thickness onlays, the test groups revealed statistically differences ($p < 0.001$) for optical transmittance at 850 nm when compared with the groups assessed before polymerization, as seen in Table 3 (supplementary material).

Regarding the analysis of the 3-mm thickness onlays, the optical transmittance of all groups was similar before and after light-curing for 40 s (after polymerization). That means a relatively small amount of light was transmitted through the 3-mm thickness onlays towards the luting materials as shown in Fig. 4D and E. The spectra behavior for 78% P was similar considering the onlay thickness and ligh-curing set. There were statistical differences for optical transmittance at 850 nm through 3-mm onlays bonded to the luting materials ($p < 0.001$), as shown in Table 4 (supplementary material).

In Fig. 5, the average ratio (Rp/np) of the light transmittance between the polymerized and non-polymerized specimens are shown regarding the light wavelength range from 400 up to 850 nm. On the 2-mm thickness onlay, the highest Rp/np ratio was measured for 60%Lf group while the 78%P revealed the lowest Rp/Np ratio ($p < 0.05$). A high Rp/np ration was also recorded for 73%B group while low Rp/np ration was measured for the thermally induced flowable resin-matrix composite reinforced with 83 wt inorganic fillers (TI83%V). On the 3-mm thickness onlay, the highest Rp/np ratio was measured for 83%Hf group, although the differences between groups were not statistically significant. A low Rp/np ratio was noticed for 3-mm thickness onlays that indicate a similarity of optical transmittance spectra regarding polymerized and non-polymerized specimens. The Rp/np ratio for specimens assessed at 850 nm is shown in Fig. 5C. There were no significant differences between 78%P specimens with 2- or 3-mm thickness onlay ($p < 0.05$). However, the values of Rp/np both for 2- mm and 3-mm thickness onlay were statistically significant ($p < 0.05$) for TI83% V group as is shown in Tables 5 and 6 (supplementary material).

3.3. Mechanical properties of the materials

In Fig. 6, the mean values and standard deviation of elastic modulus and nano-hardness are reported for the luting materials reinforced with different content of inorganic fillers.

As expected, the highest mean values of elastic modulus (21.55 ± 2.43 GPa) and nano-hardness (1.6 ± 0.13 GPa were recorded for the onlays which were composed of resin-matrix composites reinforced with 89 wt % inorganic fillers ($p < 0.001$). In the same way, flowable resin-matrix composites reinforced with 83 wt % inorganic fillers, namely 83%Lf and TI83%V groups, showed higher mean values of elastic modulus (15.1 ± 1.54 GPa and 15.7 ± 1.82 GPa, respectively) when compared with the resin-matrix cements and flowable composites containing lower content of inorganic fillers. The adhesive layer showed the lowest mean values of elastic modulus (5.44 ± 0.52 GPa) and nano-hardness (0.51 ± 0.66 GPa) followed by the materials containing 60 or 73 wt% inorganic fillers, namely 60%Lf (6.88 ± 0.64 GPa) and 73%B

Table 2
Thickness values of the specimens ($n = 10$) measured by optical microscopy. Thickness values are represented in micrometer (μm).

Group	Mean (μm)	Std	Min (μm)	Max (μm)	CI (95%)	
					I.L.	S.L.
78%P	50.56	21.19	25.40	83.40	35.40	65.72
73%B	407.23	31.47	359.40	455.40	384.72	429.74
Ti83%V	405.02	12.23	387.40	420.50	396.27	413.77
60%Lf	53.39	30.33	18.60	95.50	31.69	75.09
83%Hf	24.97	5.68	17.20	31.90	20.91	29.03

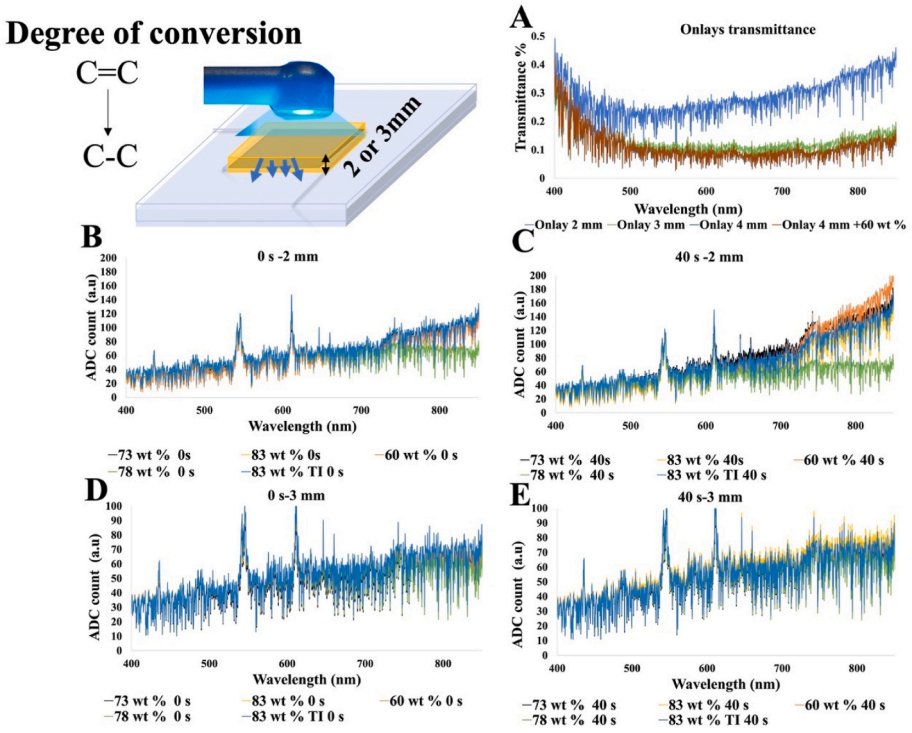

Fig. 4. (A) Optical transmittance through the onlays' specimens with thickness at 2, 3 or, 4 mm, as well through 4-mm thickness onlay bonded to a flowable resin-matrix composite reinforced with 60 wt% inorganic fillers. ADC count of the of the (B,C) 2-mm or (D,E) 3-mm thickness onlays bonded to the luting materials before and after light curing for 40 s (post-polymerization), respectively.

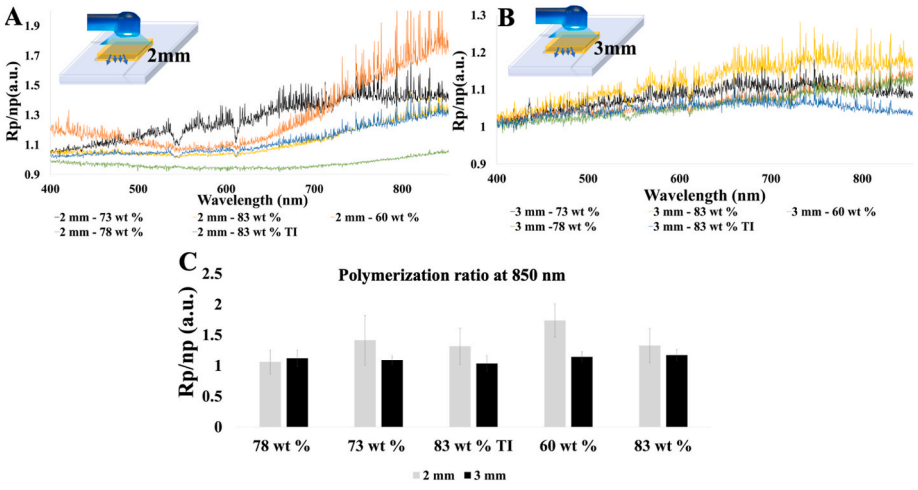

Fig. 5. Transmittance ratio (a.u.) between the polymerized and non-polymerized (Rp/np) specimens with (A) 2 mm- and (B) 3-mm thickness onlays in the wavelength range from 400 up to 850 nm at light irradiance. (C) Rp/np of all samples, measured at 850 nm.

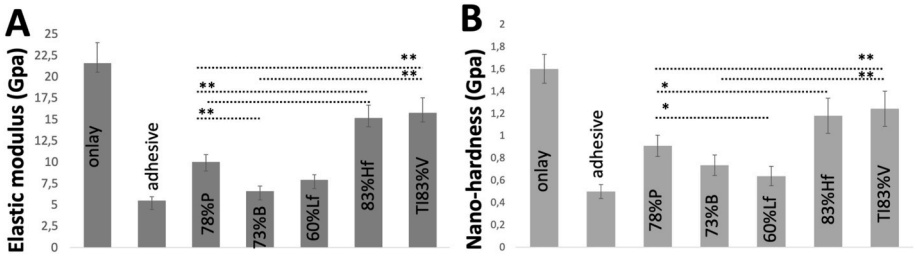

Fig. 6. (A) Elastic modulus and (B) nano-hardness recorded for the luting materials.*Statistically significant ($p < 0.05$); **Highly significant ($p < 0.001$).

(6.56 ± 0.61 GPa) groups.

4. Discussion

In this study, five different resin-matrix luting materials were analyzed by spectrophotometry and physicochemical analyses considering the variable content of inorganic filers (60, 73, 78, or 83 wt%) and applications such as traditional resin-matrix cement or restorative flowable resin-matrix composites. Thus, the findings reported in this study revealed lower light transmittance through resin-matrix composites onlay specimens with 3-mm thickness when compared to 2-mm thickness onlays. Also, the light transmittance was variable regarding the type of resin-matrix cement or flowable resin-matrix composite bonded to the onlay specimens. The chemical composition and content of the inorganic fillers affected the light transmission pathways through the interfaces. Thus, the present findings rejected the null hypothesis of this study.

The optical transmittance spectra recorded in this study increased above 600 nm reaching high values at 850 nm through the resin-matrix composites onlays, that is in accordance with other studies in literature (Lise et al., 2018b). Regarding the optical transmittance tests at 850 nm through the 2-mm thickness onlays specimens, the lowest optical transmittance was recorded for the resin-matrix cement containing 78 wt% inorganic fillers. In fact, the resin-matrix cements showed differences in their chemical composition of the organic matrix and inorganic component. As reported in other studies, the refractive indexes of monomers and inorganic fillers highly influence the optical transmittance through the materials (Fujita et al., 2005, 2011; Balbinot et al., 2019). The resin-matrix cement containing 78 wt% inorganic fillers revealed a mixture of micro-scale barium glass ceramic, fluor-aluminum-silicate, aluminum oxide, and nano-scale amorphous silica, while the resin-matrix cement containing 73 wt% involved micro-scale fluor-aluminum-silicate glass ceramic particles and nano-scale amorphous silica. The light transmittance was similar for the resin-matrix cement with 73 wt% inorganic fillers and thermally induced flowable resin-matrix composite with 83 wt% inorganic fillers. The flowable resin-matrix composites containing 83 wt% showed inorganic particles composed of micro-scale zirconium glass and nano-scale amorphous silica with similar shape and size. The highest optical transmittance values and Rp/np ratio were recorded for the flowable resin-matrix composite with 60 wt% inorganic fillers, namely micro-scale zinc oxide and nano-scale amorphous silica, due to its lowest inorganic content. That flowable resin-matrix composites revealed micro-scale zinc oxide and nano-scale amorphous silica. The findings revealed that a lower content of inorganic particles decreases the light scattering phenomena which occurs through interfaces with a high content of inorganic fillers. Such findings are in agreement with other studies reported in literature (Tomaselli et al., 2019; Masotti et al., 2007; Howard et al., 2010; Arikawa et al., 1998; Fidalgo-Pereira et al., 2023).

The chemical composition of the materials was given by the manufacturers although differences in the microstructure of the materials were detailly examined by SEM coupled to energy dispersive spectroscopy, as seen in Fig. 2. At first, inorganics fillers of the resin-matrix luting materials were inspected and measured revealing different types of fillers and variable dimensions for each material. All the materials revealed micro-scale glass fillers with irregular shape embedded within the organic matrix (Fig. 2). The high content of fillers in the microstructure of the materials is industrially achieved by the variable size from micro-scale down to submicron- or nano-scale size of the particles. Also, the size and shape of the inorganic fillers determine the viscosity and flowing of the materials over the cementation procedure leading to an adequate cement layer at the restorative interfaces (Magalhães et al., 2023; May et al., 2015; Alrahlah et al., 2014; Gugelmin et al., 2020).

The results revealed that the light was not transmitted through the specimen with 4-mm thickness and therefore the specimens were withdrawn for further light transmittance assays involving the luting materials. The light transmittance spectra were lower for 3-mm thickness onlays specimens than that recorded for 2-mm thickness onlays. Such results are in accordance with the results reported in previous studies considering light irradiance is lower through the luting materials as the restorative thickness increases (Okutan et al., 2022a, 2022b; Ilie, 2017; Lee et al., 2008). The high content of inorganic fillers (89 wt%) composed of micro-scale barium glass ceramics, zirconium silicate glass ceramics, and nano-scale amorphous silica of the resin-composite onlays produced for CAD-CAM influenced the optical transmittance towards the luting materials (Lise et al., 2018b; Shortall et al., 2008). The increase in the onlay thickness also increased the overall refractive index of monomers and inorganic fillers that influence the light transmittance through onlays and luting materials (Hardy et al., 2018, 2021). Indeed, a high refractive index block the light transmission towards the restorative interface. Indirect restorative thicknesses must be carefully controlled, since the restoration material can absorb, reflect, or refract the light leading to insufficient amount of light over the luting materials (De Angelis et al., 2021). On the 3-mm thickness onlays, the lowest light transmittance and Rp/np values were recorded for the thermally induced resin-matrix composites reinforced with 83 wt% inorganic fillers. The thickness of indirect restorative materials highly influences the light transmittance through the restorative material leading to a low light irradiance towards the luting material (Babaier et al., 2022; Caprak et al., 2019). Thus, the occlusal region has mean thickness values of around 2 mm mainly regarding inlay restorations. However, the onlay restorative material can reach a thickness of 3 mm on the proximal regions and therefore the light irradiance from the LCU unit comes from the occlusal towards the proximal margins to reach the resin cement at the deepest regions. A low light irradiance is detrimental to the degree of conversion (DC) of monomers that results in poor physical properties and release of toxic molecules to the surrounding environment. The findings on the Rp/np ratio and the low optical transmittance after polymerization indicate that dual-curing resin cements are recommended for thick restorative structures above 2-mm thickness as reported in the literature (Acquaviva et al., 2009; Supornpun et al., 2023; Babaier et al., 2022). In the dual-curing polymerization, the chemically-induced reaction occurs after the light-induced reaction and the viscosity of the organic matrix does not increase promptly as occurs in solely light-curing materials. Then, the DC of monomers in the organic matrix of those is dependent on the chemical reaction to achieve the suitable mechanical properties for the luting materials (Aldhafyan et al., 2021; Yang et al., 2020). On polymerization, DC of monomers involves the amount of double carbon bonds (C═C) remaining after polymerization, compared to the total number of C═C of the unpolymerized material. The differences in optical transmittance, regarding the resin-matrix cements and the resin-matrix composites, can also be explained by the differences on the initiator's chemistry (Lise et al., 2018b; Chen et al., 2019; Fidalgo-Pereira et al., 2023). The use of light cured materials with thick indirect restorations (thicker than 2 mm), must be restricted to translucid materials, such as glass ceramic veneers (Hardy et al., 2021; Gregor et al., 2014; Shim et al., 2017; Yoshida and Meng, 2014).

The influence of multiple variables on the optical transmittance and, consequently, on the DC of resin-matrix luting materials were noticed in the present study. The type of luting material (de Castro et al., 2023; Oh et al., 2018b; Pacheco et al., 2019; Shim et al., 2017) and the thickness of the indirect restorative material (Moreno et al., 2018; Öztürk et al., 2013; Gregor et al., 2014) were determinant factors for the differences found between the tested materials. Thus, the relationship among light irradiance, polymerization mode, materials, restorative thickness, DC, and chemical composition plays an important role on the physicochemical behavior of the restorative interfaces. The present findings were validated considering the differences in light transmittance through the tested groups of resin-matrix luting materials with inorganic fillers ranging from 60 up 83 wt%. Despite the study limitations, the

reported results are clinically relevant concerning light-cured resin--matrix composites may not receive enough light irradiance and energy for polymerization through thick restorative onlays. The present results bring relevant data for the clinicians once a proper selection of materials and thickness of restorative materials provide the desirable physical properties of the restorative interfaces in the oral environment (Fujita et al., 2005; Ling et al., 2022; Pacheco et al., 2019). Commercially availabe resin-matrix luting materials are increasingly improved by manufacturers and a widespread number of novel materials are available for restorative dentistry. Then, novel materials must be examined by traditional and alternative physicochemical approaches. Visible and near-IR spectrophotometry could be considered as a potential alternative methodology to estimate the DC of resin-matrix luting materials by assessing the light transmittance behavior. Further studies can be carried out involving a comparison of results with other methods such as Fourier transform infrared (FTIR) or near infrared (NIR). Furthermore, future studies should examine different light exposure times, restorative materials, and examine the DC along several time points after polymerization, to reveal a direct influence on the clinical behavior of the restorative interfaces. Additionally, different materials could be tested concerning the behavior of the restorative interfaces involving translucid or opaque materials (Kelch et al., 2022b).

Considering the findings from the present study, dual-cured resin-matrix cements must be considered for cementation of thick restorative materials. Nevertheless, further studies are required for evaluating different parameters involving light curing mode, microstructure, and polymerization of recent resin-matrix cements and flowable resin-matrix composites.

5. Conclusions

The present results revealed that the light transmittance decreased with the increase of the composite onlay thickness from 2 up to 3 mm leading to a low amount of visible light for inducing the polymerization of resin-matrix luting materials. Additionally, the microstructure of the resin-matrix cements and composites involved a high content of micro- and nano-scale inorganic fillers that influence the absorption and refraction of light. As a result, a high overall light refractive index deceased the light transmittance through the onlays causing inefficient degree of conversion of the organic matrix of the resin-matrix cements and flowable composites.

Author contributions

Annabel Braem: Writing – review & editing, Methodology, Investigation, Funding acquisition, Formal analysis, Data curation. Julio Souza: Writing – review & editing, Validation, Supervision, Resources, Project administration, Investigation, Funding acquisition, Data curation, Conceptualization. Susana Catarino: Validation, Software, Data curation. Óscar Carvalho: Visualization, Validation, Methodology, Investigation, Data curation. Nélio Veiga: Validation, Software, Data curation. Orlanda Torres: Supervision, Investigation, Conceptualization. Rita Fidalgo-Pereira: Writing – original draft, Investigation

Funding

This work was supported by the following FCT projects: UIDB/04436/2020 and UIDP/04436/2020, PTDC/EMEEME/4197/2021, and 2020.00215.CEECIND.

Declaration of competing interest

The authors declare the following financial interests/personal relationships which may be considered as potential competing interests: The authors declare no conflict of interest.

The authors report financial support was provided by Foundation for Science and Technology.

Data availability

Data will be made available on request.

Acknowledgments

The authors acknowledge financial support provided by the Portuguese Foundation for Science and Technology (FCT) and KU Leuven (Belgium). The authors also acknowledge VOCO GmbH for the support and providing resin-matrix composites materials for the development of this study.

Appendix A. Supplementary data

Supplementary data to this article can be found online at https://doi.org/10.1016/j.jmbbm.2023.106353.

References

Acquaviva, P.A., Cerutti, F., Adami, G., Gagliani, M., Ferrari, M., Gherlone, E., et al., 2009. Degree of conversion of three composite materials employed in the adhesive cementation of indirect restorations: a micro-Raman analysis. J. Dent. 37, 610–615. https://doi.org/10.1016/j.jdent.2009.04.001.

Aguiar, T.R., Di Francescantonio, M., Bedran-Russo, A.K., Giannini, M., 2012. Inorganic composition and filler particles morphology of conventional and self-adhesive resin cements by SEM/EDX. Microsc. Res. Tech. 75, 1348–1352. https://doi.org/10.1002/jemt.22073.

Aldhafyan, M., Silikas, N., Watts, D.C., 2021. Influence of curing modes on thermal stability, hardness development and network integrity of dual-cure resin cements. Dent. Mater. 37, 1854–1864. https://doi.org/10.1016/j.dental.2021.09.016.

Alkhudhairy, F., Vohra, F., Naseem, M., Owais, M.M., Amer, A.H.B., Almutairi, K.B., 2020. Color stability and degree of conversion of a novel dibenzoyl germanium derivative containing photo-polymerized resin luting cement. J. Appl. Biomater. Funct. Mater. 18, 2280800020917326 https://doi.org/10.1177/2280800020917326.

Alrahlah, A., Silikas, N., Watts, D.C., 2014. Hygroscopic expansion kinetics of dental resin-composites. Dent. Mater. 30, 143–148. https://doi.org/10.1016/j.dental.2013.10.010.

Arikawa, H., Fujii, K., Kanie, T., Inoue, K., 1998. Optical transmittance characteristics of light-cured composite resins. Dent. Mater. 14, 405–411. https://doi.org/10.1016/s0300-5712(99)00014-7.

Babaier, R., Haider, J., Silikas, N., Watts, D.C., 2022. Effect of CAD/CAM aesthetic material thickness and translucency on the polymerisation of light- and dual-cured resin cements. Dent. Mater. 38, 2073–2083. https://doi.org/10.1016/j.dental.2022.11.016.

Balbinot, E., Pereira, M., Skupien, J.A., Balbinot, C.E.A., da Rocha, G., Vieira, S., 2019. Analysis of transmittance and degree of conversion of composite resins. Microsc. Res. Tech. 82, 1953–1961. https://doi.org/10.1002/jemt.23364.

Barbon, F.J., Isolan, C.P., Soares, L.D., Bona, A.D., de Oliveira da Rosa, W.L., Boscato, N., 2022. A systematic review and meta-analysis on using preheated resin composites as luting agents for indirect restorations. Clin. Oral Invest. 26, 3383–3393. https://doi.org/10.1007/s00784-022-04406-z.

Blumentritt, F.B., Cancian, G., Saporiti, J.M., de Holanda, T.A., Barbon, F.J., Boscato, N., 2021. Influence of feldspar ceramic thickness on the properties of resin cements and restorative set. Eur. J. Oral Sci. 129, e12765 https://doi.org/10.1111/eos.12765.

Bragança, G.F., Vianna, A.S., Neves, F.D., Price, R.B., Soares, C.J., 2020. Effect of exposure time and moving the curing light on the degree of conversion and Knoop microhardness of light-cured resin cements. Dent. Mater. 36, e340–e351. https://doi.org/10.1016/j.dental.2020.08.016.

Butler, S., Santos, G.C., Santos, M.J.C., 2021. Do high translucency zirconia shades contribute to the degree of conversion of dual-cure resin cements? Quintessence Int. 53, 8–14. https://doi.org/10.3290/j.qi.b1901343.

Caprak, Y.O., Turkoglu, P., Akgungor, G., 2019. Does the translucency of novel monolithic CAD/CAM materials affect resin cement polymerization with different curing modes? J. Prosthodont. 28, e572–e579. https://doi.org/10.1111/jopr.12956.

Chen, Y., Yao, C., Huang, C., Wang, Y., 2019. The effect of monowave and polywave light-polymerization units on the adhesion of resin cements to zirconia. J. Prosthet. Dent 121, 549.e1–549.e7. https://doi.org/10.1016/j.prosdent.2018.12.010.

David-Pérez, M., Ramírez-Suárez, J.P., Latorre-Correa, F., Agudelo-Suárez, A.A., 2022. Degree of conversion of resin-cements (light-cured/dual-cured) under different thicknesses of vitreous ceramics: systematic review. J Prosthodont Res 66, 385–394. https://doi.org/10.2186/jpr.JPR_D_20_00090.

De Angelis, F., Vadini, M., Capogreco, M., D'arcangelo, C., D'amario, M., 2021. Effect of light-sources and thicknesses of composite onlays on micro-hardness of luting composites. Materials 14. https://doi.org/10.3390/ma14226849.

de Castro, E.F., Fronza, B.M., Soto-Montero, J., Giannini, M., dos-Santos-Dias, C.T., Price, R.B., 2023. Effect of thickness of CAD/CAM materials on light transmission

and resin cement polymerization using a blue light-emitting diode light-curing unit. J. Esthetic Restor. Dent. 35, 368–380. https://doi.org/10.1111/jerd.12946.
De Souza, G., Braga, R.R., Cesar, P.F., Lopes, G.C., 2015. Correlation between clinical performance and degree of conversion of resin cements: a literature review. J. Appl. Oral Sci. 23, 358–368. https://doi.org/10.1590/1678-775720140524.
Delgado, A.J., Castellanos, E.M., Sinhoreti, M., Oliveira, D.C., Abdulhameed, N., Geraldeli, S., et al., 2019. The use of different photoinitiator systems in photopolymerizing resin cements through ceramic veneers. Operat. Dent. 44, 396–404. https://doi.org/10.2341/17-263-l.
El-Safty, S., Akhtar, R., Silikas, N., Watts, D.C., 2012. Nanomechanical properties of dental resin-composites. Dent. Mater. 28, 1292–1300. https://doi.org/10.1016/j.dental.2012.09.007.
Faria, E.S.A.L., Pfeifer, C.S., 2017. Effectiveness of high-power LEDs to polymerize resin cements through ceramics: an in vitro study. J. Prosthet. Dent 118, 631–636. https://doi.org/10.1016/j.prosdent.2016.12.013.
Ferracane, J.L., Stansbury, J.W., Burke, F.J., 2011. Self-adhesive resin cements - chemistry, properties and clinical considerations. J. Oral Rehabil. 38, 295–314. https://doi.org/10.1111/j.1365-2842.2010.02148.x.
Fidalgo-Pereira, R., Carpio, D., Torres, O., Carvalho, O., Silva, F., Henriques, B., et al., 2022. The influence of inorganic fillers on the light transmission through resin-matrix composites during the light-curing procedure: an integrative review. Clin. Oral Invest. https://doi.org/10.1007/s00784-022-04589-5.
Fidalgo-Pereira, R., Carvalho, O., Catarino, S.O., Henriques, B., Torres, O., Braem, A., Souza, J.C.M., 2023. Effect of inorganic fillers on the light transmission through traditional or flowable resin-matrix composites for restorative dentistry. Clin. Oral. Investig. Sep 27 (9), 5679–5693. https://doi.org/10.1007/s00784-023-05189-7.
Fidalgo-Pereira, R., Torres, O., Carvalho, Ó., Silva, F.S., Catarino, S.O., Özcan, M., et al., 2023. A scoping review on the polymerization of resin-matrix cements used in restorative dentistry. Materials 16, 1560.
Franken, P., Rodrigues, S.B., Collares, F.M., Samuel, S.M.W., Leitune, V.C.B., 2019. Influence of N-(2-hydroxyethyl)acrylamide addition in light- and dual-cured resin cements. J. Dent. 90, 103208 https://doi.org/10.1016/j.jdent.2019.103208.
Fujita, K., Nishiyama, N., Nemoto, K., Okada, T., Ikemi, T., 2005. Effect of base monomer's refractive index on curing depth and polymerization conversion of photo-cured resin composites. Dent. Mater. J. 24, 403–408. https://doi.org/10.4012/dmj.24.403.
Fujita, K., Ikemi, T., Nishiyama, N., 2011. Effects of particle size of silica filler on polymerization conversion in a light-curing resin composite. Dent. Mater. 27, 1079–1085. https://doi.org/10.1016/j.dental.2011.07.010.
Gheller, R., Burey, A., Vicentin, B.L.S., Dos Reis, P.J., Appoloni, C.R., Garbelini, C.C.D., et al., 2020. Microporosity and polymerization contraction as function of depth in dental resin cements by X-ray computed microtomography. Microsc. Res. Tech. 83, 658–666. https://doi.org/10.1002/jemt.23456.
Goel, D., Sandhu, M., Jhingan, P., Sachdev, V., 2013. Sensitivity and Specificity of Air-Drying and Magnification in Detection of Initial Caries on Occlusal Surfaces, vol. 40.
Goldberg, J., Güth, J.-F., Magne, P., 2016. Accelerated fatigue resistance of thick CAD/CAM composite resin overlays bonded with light- and dual-polymerizing luting resins. J. Adhesive Dent. 18, 341–348. https://doi.org/10.3290/j.jad.a36515.
González-Colmenares, G., Calvo-Díaz, L., Nastul-Enríquez, M., Bertel-Ruíz, M.M., Garzón-Ramírez, I., Rojas-Sánchez, M.P., et al., 2020. Effect of high temperatures on teeth fixed with an orthodontic bracket. An in vitro study. Forensic Sci. Int. 308, 110182 https://doi.org/10.1016/j.forsciint.2020.110182.
Gregor, L., Bouillaguet, S., Onisor, I., Ardu, S., Krejci, I., Rocca, G.T., 2014. Microhardness of light- and dual-polymerizable luting resins polymerized through 7.5-mm-thick endocrowns. J. Prosthet. Dent 112, 942–948. https://doi.org/10.1016/j.prosdent.2014.02.008.
Gugelmin, B.P., Miguel, L.C.M., Baratto Filho, F., Cunha, LF da, Correr, G.M., Gonzaga, C.C., 2020. Color stability of ceramic veneers luted with resin cements and pre-heated composites: 12 Months follow-up. Braz. Dent. J. 31.
Gultekin, P., Pak Tunc, E., Ongul, D., Turp, V., Bultan, O., Karataslı, B., 2015. Curing efficiency of dual-cure resin cement under zirconia with two different light curing units. J. Istanbul Univ. Fac. Dent. 49, 8–16. https://doi.org/10.17096/jiufd.97059.
Hardy, C.M.F., Bebelman, S., Leloup, G., Hadis, M.A., Palin, W.M., Leprince, J.G., 2018. Investigating the limits of resin-based luting composite photopolymerization through various thicknesses of indirect restorative materials. Dent. Mater. 34, 1278–1288. https://doi.org/10.1016/j.dental.2018.05.009.
Hardy, C.M.F., Leprince, J., Landreau, V., Valassis, M., Mercelis, B., de Munck, J., et al., 2021. Mini-iFT confirms superior adhesive luting performance using light-curing restorative composites. J. Adhesive Dent. 23, 539–548. https://doi.org/10.3290/j.jad.b2287755.
Howard, B., Wilson, N.D., Newman, S.M., Pfeifer, C.S., Stansbury, J.W., 2010. Relationships between conversion, temperature and optical properties during composite photopolymerization. Acta Biomater. 6, 2053–2059. https://doi.org/10.1016/j.actbio.2009.11.006.
Ilie, N., 2017. Transmitted irradiance through ceramics: effect on the mechanical properties of a luting resin cement. Clin. Oral Invest. 21, 1183–1190. https://doi.org/10.1007/s00784-016-1891-3.
Ioannidis, A., Mühlemann, S., Özcan, M., Hüsler, J., Hämmerle, C.H.F., Benic, G.I., 2019. Ultra-thin occlusal veneers bonded to enamel and made of ceramic or hybrid materials exhibit load-bearing capacities not different from conventional restorations. J. Mech. Behav. Biomed. Mater. 90, 433–440. https://doi.org/10.1016/j.jmbbm.2018.09.041.
Kameyama, A., Bonroy, K., Elsen, C., Lührs, A.-K., Suyama, Y., Peumans, M., et al., 2015. Luting of CAD/CAM ceramic inlays: direct composite versus dual-cure luting cement. Bio Med. Mater. Eng. 25 https://doi.org/10.3233/BME-151274, 279–88.
Kelch, M., Stawarczyk, B., Mayinger, F., 2022a. Time-dependent degree of conversion, Martens parameters, and flexural strength of different dual-polymerizing resin composite luting materials. Clin. Oral Invest. 26, 1067–1076. https://doi.org/10.1007/s00784-021-04091-4.
Kelch, M., Stawarczyk, B., Mayinger, F., 2022b. Time-dependent degree of conversion, Martens parameters, and flexural strength of different dual-polymerizing resin composite luting materials. Clin. Oral Invest. 26, 1067–1076. https://doi.org/10.1007/s00784-021-04091-4.
Kim, M.J., Kim, K.H., Kim, Y.K., Kwon, T.Y., 2013. Degree of conversion of two dual-cured resin cements light-irradiated through zirconia ceramic disks. Journal of Advanced Prosthodontics 5, 464–470. https://doi.org/10.4047/jap.2013.5.4.464.
Lee, I.B., An, W., Chang, J., Um, C.M., 2008. Influence of ceramic thickness and curing mode on the polymerization shrinkage kinetics of dual-cured resin cements. Dent. Mater. 24, 1141–1147. https://doi.org/10.1016/j.dental.2008.03.015.
Ling, L., Ma, Y., Chen, Y., Malyala, R., 2022. Physical, mechanical, and adhesive properties of novel self-adhesive resin cement. Int J Dent 2022, 4475394. https://doi.org/10.1155/2022/4475394.
Lise, D.P., Van Ende, A., De Munck, J., Yoshihara, K., Nagaoka, N., Cardoso Vieira, L.C., et al., 2018a. Light irradiance through novel CAD-CAM block materials and degree of conversion of composite cements. Dent. Mater. 34, 296–305. https://doi.org/10.1016/j.dental.2017.11.008.
Lise, D.P., Van Ende, A., De Munck, J., Yoshihara, K., Nagaoka, N., Cardoso Vieira, L.C., et al., 2018b. Light irradiance through novel CAD-CAM block materials and degree of conversion of composite cements. Dent. Mater. 34, 296–305. https://doi.org/10.1016/j.dental.2017.11.008.
Magalhães, T., Fidalgo-Pereira, R., Torres, O., Carvalho, Ó., Silva, F.S., Henriques, B., et al., 2023. Microscopic inspection of the adhesive interface of composite onlays after cementation on low loading: an in vitro study. J. Funct. Biomater. 14, 148. https://doi.org/10.3390/jfb14030148.
Magne, P., Knezevic, A., 2009. Simulated fatigue resistance of composite resin versus porcelain CAD/CAM overlay restorations on endodontically treated molars. Quintessence Int. 40, 125–133.
Masotti, A.S., Onófrio, A.B., Conceição, E.N., Spohr, A.M., 2007. UV-vis spectrophotometric direct transmittance analysis of composite resins. Dent. Mater. 23, 724–730. https://doi.org/10.1016/j.dental.2006.06.020.
May, L.G., Robert Kelly, J., Bottino, M.A., Hill, T., 2015. Influence of the resin cement thickness on the fatigue failure loads of CAD/CAM feldspathic crowns. Dent. Mater. 31, 895–900. https://doi.org/10.1016/j.dental.2015.04.019.
Mazzitelli, C., Maravic, T., Mancuso, E., Josic, U., Generali, L., Comba, A., et al., 2022. Influence of the activation mode on long-term bond strength and endogenous enzymatic activity of dual-cure resin cements. Clin. Oral Invest. 26, 1683–1694. https://doi.org/10.1007/s00784-021-04141-x.
Mendonça, L.M., Ramalho, I.S., Lima, L., Pires, L.A., Pegoraro, T.A., Pegoraro, L.F., 2019. Influence of the composition and shades of ceramics on light transmission and degree of conversion of dual-cured resin cements. J. Appl. Oral Sci. 27, e20180351 https://doi.org/10.1590/1678-7757-2018-0351.
Meng, K., Wang, L., Wang, J., Yan, Z., Zhao, B., Li, B., 2022. Effect of optical properties of lithium disilicate glass ceramics and light-curing protocols on the curing performance of resin cement. Coatings 12, 715.
Moldovan, M., Balazsi, R., Soanca, A., Roman, A., Sarosi, C., Prodan, D., et al., 2019. Evaluation of the degree of conversion, residual monomers and mechanical properties of some light-cured dental resin composites. Materials 12. https://doi.org/10.3390/ma12132109.
Moreno, M.B.P., Costa, A.R., Rueggeberg, F.A., Correr, A.B., Sinhoreti, M.A.C., Ambrosano, G.M.B., et al., 2018. Effect of ceramic interposition and post-activation times on knoop hardness of different shades of resin cement. Braz. Dent. J. 29.
Oh, S., Shin, S.M., Kim, H.J., Paek, J., Kim, S.J., Yoon, T.H., et al., 2018a. Influence of glass-based dental ceramic type and thickness with identical shade on the optical transmittance and the degree of conversion of resin cement. Int. J. Oral Sci. 10, 5. https://doi.org/10.1038/s41368-017-0005-7.
Oh, S., Shin, S.-M., Kim, H.-J., Paek, J., Kim, S.-J., Yoon, T.H., et al., 2018b. Influence of glass-based dental ceramic type and thickness with identical shade on the optical transmittance and the degree of conversion of resin cement. Int. J. Oral Sci. 10, 5. https://doi.org/10.1038/s41368-017-0005-7.
Okutan, Y., Kandemir, B., Donmez, M.B., Yucel, M.T., 2022a. Effect of the thickness of CAD-CAM materials on the shear bond strength of light-polymerized resin cement. Eur. J. Oral Sci. 130, e12892 https://doi.org/10.1111/eos.12892.
Okutan, Y., Kandemir, B., Donmez, M.B., Yucel, M.T., 2022b. Effect of the thickness of CAD-CAM materials on the shear bond strength of light-polymerized resin cement. Eur. J. Oral Sci. 130, e12892 https://doi.org/10.1111/eos.12892.
Öztürk, E., Chiang, Y.-C., Coşgun, E., Ş, Bolay, Hickel, R., Ilie, N., 2013. Effect of resin shades on opacity of ceramic veneers and polymerization efficiency through ceramics. J. Dent. 41, e8–e14. https://doi.org/10.1016/j.jdent.2013.06.001.
Pacheco, R.R., Carvalho, A.O., André, C.B., Ayres, A.P.A., de Sá, R.B.C., Dias, T.M., et al., 2019. Effect of indirect restorative material and thickness on light transmission at different wavelengths. J Prosthodont Res 63, 232–238. https://doi.org/10.1016/j.jpor.2018.12.004.
Rode, K.M., Kawano, Y., Turbino, M.L., 2007. Evaluation of curing light distance on resin composite microhardness and polymerization. Operat. Dent. 32, 571–578. https://doi.org/10.2341/06-163.
Sadighpour, L., Geramipanah, F., Ghasri, Z., Neshatian, M., 2018. Microtensile bond strength of CAD/CAM-fabricated polymer-ceramics to different adhesive resin cements. Restor Dent Endod 43, e40. https://doi.org/10.5395/rde.2018.43.e40.
Santi, M.R., Lins, R.B.E., Sahadi, B.O., Denucci, G.C., Soffner, G., Martins, L.R.M., 2022. Influence of inorganic composition and filler particle morphology on the mechanical

properties of self-adhesive resin cements. Restor Dent Endod 47, e32. https://doi.org/10.5395/rde.2022.47.e32.

Shim, J.S., Kang, J.K., Jha, N., Ryu, J.J., 2017. Polymerization mode of self-adhesive, dual-cured dental resin cements light cured through various restorative materials. J. Esthetic Restor. Dent. 29, 209–214. https://doi.org/10.1111/jerd.12285.

Shortall, A.C., Palin, W.M., Burtscher, P., 2008. Refractive index mismatch and monomer reactivity influence composite curing depth. J. Dent. Res. 87, 84–88. https://doi.org/10.1177/154405910808700115.

Souza, J.C., Henriques, B., Ariza, E., Martinelli, A.E., Nascimento, R.M., Silva, F.S., et al., 2014. Mechanical and chemical analyses across dental porcelain fused to CP titanium or Ti6Al4V. Mater. Sci. Eng., C 37, 76–83. https://doi.org/10.1016/j.msec.2013.12.030.

Straface, A., Rupp, L., Gintaute, A., Fischer, J., Zitzmann, N.U., Rohr, N., 2019. HF etching of CAD/CAM materials: influence of HF concentration and etching time on shear bond strength. Head Face Med. 15, 21. https://doi.org/10.1186/s13005-019-0206-8.

Sulaiman, T.A., Abdulmajeed, A.A., Donovan, T.E., Ritter, A.V., Lassila, L.V., Vallittu, P. K., et al., 2015. Degree of conversion of dual-polymerizing cements light polymerized through monolithic zirconia of different thicknesses and types. J. Prosthet. Dent 114, 103–108. https://doi.org/10.1016/j.prosdent.2015.02.007.

Supornpun, N., Oster, M., Phasuk, K., Chu, T.-M.G., 2023. Effects of shade and thickness on the translucency parameter of anatomic-contour zirconia, transmitted light intensity, and degree of conversion of the resin cement. J. Prosthet. Dent 129, 213–219. https://doi.org/10.1016/j.prosdent.2021.04.019.

Tafur-Zelada, C.M., Carvalho, O., Silva, F.S., Henriques, B., Özcan, M., Souza, J.C.M., 2021. The influence of zirconia veneer thickness on the degree of conversion of resin-matrix cements: an integrative review. Clin. Oral Invest. 25, 3395–3408. https://doi.org/10.1007/s00784-021-03904-w.

Tekçe, N., Tuncer, S., Demirci, M., 2018. The effect of sandblasting duration on the bond durability of dual-cure adhesive cement to CAD/CAM resin restoratives. J Adv Prosthodont 10, 211–217. https://doi.org/10.4047/jap.2018.10.3.211.

Tomaselli, L.O., Oliveira, D.C.R.S., Favarão, J., Silva, A.F.D., Pires-de-Souza, F.C.P., Geraldeli, S., Sinhoreti, M.A.C., 2019. Influence of pre-heating regular resin composites and flowable composites on luting ceramic veneers with different thicknesses. Braz. Dent. J. 30 (5), 459–466. https://doi.org/10.1590/0103-6440201902513.

Turp, V., Ongul, D., Gultekin, P., Bultan, O., Karataslı, B., Pak Tunc, E., 2015. Polymerization efficiency of two dual-cure cements through dental ceramics. J. Istanbul Univ. Fac. Dent. 49, 10–18. https://doi.org/10.17096/jiufd.25575.

Valentini, F., Moraes, R.R., Pereira-Cenci, T., Boscato, N., 2014. Influence of glass particle size of resin cements on bonding to glass ceramic: SEM and bond strength evaluation. Microsc. Res. Tech. 77, 363–367. https://doi.org/10.1002/jemt.22353.

Valentino, T.A., Borges, G.A., Borges, L.H., Vishal, J., Martins, L.R., Correr-Sobrinho, L., 2010. Dual resin cement knoop hardness after different activation modes through dental ceramics. Braz. Dent. J. 21, 104–110. https://doi.org/10.1590/s0103-64402010000200003.

Xu, T., Li, X., Wang, H., Zheng, G., Yu, G., Wang, H., et al., 2020. Polymerization shrinkage kinetics and degree of conversion of resin composites. J. Oral Sci. 62, 275–280. https://doi.org/10.2334/josnusd.19-0157.

Yang, B., Huang, Q., Holmes, B., Guo, J., Li, Y., Heo, Y., et al., 2020. Influence of curing modes on the degree of conversion and mechanical parameters of dual-cured luting agents. J Prosthodont Res 64, 137–144. https://doi.org/10.1016/j.jpor.2019.06.002.

Yoshida, K., Meng, X., 2014. Microhardness of dual-polymerizing resin cements and foundation composite resins for luting fiber-reinforced posts. J. Prosthet. Dent 111, 505–511. https://doi.org/10.1016/j.prosdent.2013.07.023.

Zhang, L., Luo, X.P., Tan, R.X., 2019. Effect of light-cured resin cement application on translucency of ceramic veneers and light transmission of LED polymerization units. J. Prosthodont. 28, e376–e382. https://doi.org/10.1111/jopr.12910.

Zimmermann, M., Ender, A., Egli, G., Özcan, M., Mehl, A., 2019. Fracture load of CAD/CAM-fabricated and 3D-printed composite crowns as a function of material thickness. Clin. Oral Invest. 23, 2777–2784. https://doi.org/10.1007/s00784-018-2717-2.